Large Eddy Simulation of transitional boundary layer flow on wind turbine blade

Z. JING[a], A. DUCOIN[b]

a. Laboratoire LHEEA, Ecole Centrale de Nantes (CNRS UMR 6598), 44300 Nantes, France , Nantes, zhenrong.jing@ec-nantes.fr

b. Laboratoire LHEEA, Ecole Centrale de Nantes (CNRS UMR 6598), 44300 Nantes, France , Nantes, antoine.ducoin@ec-nantes.fr

Résumé :

Du a leur grande échelle, les éoliennes à axe horizontales opèrent classiquement à haut nombre de Reynolds. Cependant, il à été montré que la transition laminaire turbulent pouvait apparaître à la surface des pales, ce qui a pour effet d'augmenter la traînée de frottement, et ainsi affecter les performances de la turbine. Cet article a pour objectif d'étudier l'écoulement de couche limite instable sur une pale d'éolienne avec une approche Large Eddy Simulation (LES), afin de quantifier son influence sur les performances globales. Le code open source Nek5000 est utilisé, qui est basé sur la méthode aux elements spectraux. Nous introduisons une technique de moyennage au sein de chaque éléments à ordre élevé afin de stabiliser les simulation LES. La méthode est tout d'abord testée sur le cas de la plaque plane transitionelle. Les résultats sont en bon accord avec la littérature, ainsi qu'avec une DNS pleinement résolue. Une LES sur une éoliennes NM80 avec une vitesse angulaire de 1.8rad/s est ensuite effectuée. Le modèle d'éolienne est le même que pour le projet DAN-AERI MW [1]. La simulation prends en compte les effets de la rotation de la turbine, et capture l'écoulement de couche limite instable sur une portion de la pale. La physique de transition et son influence sur les performances est étudiée.

Abstract :

Wind turbines usually operate at large Reynolds number. However, even under those conditions, laminar-turbulent transition can happens at the blade surface, which increases the frictional drag and might affect the performance of the turbines. This paper aimes to study boundary layer transition on wind turbine blades by Large Eddy Simulation(LES), and quantify its influence on wind turbine performance. The open-source code Nek5000, which is based Spectral Element Method, is used in this study. It has spectral convergence rate and low numerical dissipation. The dynamic Smagrinsky model was developed in the code. In this paper, we introduce a element-wise averaging technique to make the LES simulation stable in the spectral element method (SEM). The LES model was first tested with a transitional flat plat boundary layer flow. The results agree well with Direct Numberical Simulation (DNS) in terms of friction coefficient, transition location and flow profiles. LES on a NM80 turbine with angular velocity 1.8rad/s is then performed. The turbine model is the same as the DAN-AERO MW project [1]. The simulation takes the rotating effects into consideration, and fully captures the boundary layer laminar-turbulent transition over a part of the blade span. The transition process and its influence on the wind turbine performance is assessed.

Mots clefs : Large Eddy Simulation, Laminar-Turbulent Transition, Wind Turbine Blades, Rotation effect

1 Introduction

Typical horizontal axis wind turbine (HAWT) blade is made up by a series of airfoil cross-section. Similar to the flow around a 2D airfoil, laminar-turbulent transition can effect the friction drag, stall, flow separation, and eventually the turbine performance. It is getting more attention as the advent of new experimental technologies and increasing computational capacity make it possible to make investigations which were impossible in the past [1].
Computational Fluid Dynamic (CFD) is widely used in the wind turbine design. However, due to the large scale of the HAWT and the resulted high Reynolds number, it is still quite challenging (if not impossible) to obtain all the flow details on the wind turbine blades, and to get a detailed wake at the same time. There are two different strategies to simulate the flow around HAWT through CFD. The first strategy is to model the turbine using actuator methods (for example actuator disk or actuator lines), and resolve the wake with advanced CFD techniques such as Large Eddy Simulation (LES) or Detached Eddy Simulation (DES), see [9, 10]. The other popular method is to fully model the wind turbine, or at least one full blade using periodic boundary conditions. However, because of the high Reynolds number, most of the existing studies rely on Reynolds Averaged Navier-Stokes (RANS) methods and focus on the pressure distribution or total lift and drag, with limited delails abount the boundary layer flow [13]. However, few studies have attempted to solve for the flow around the blades using DES techniques, see [12, 14]. The results suggest that the boundary layer flow around a blade in rotation may differ from a quasi 2D flow around an airfoil, which is classicaly investigated [7].

This paper aims to provide a fully resolved Large Eddy Simulation (LES) of the boundary layer flow on a rotating wind turbine blade. We are mainly interested in :(1) details of flow transition, (2)effect of rotation on the transition; (3) the influence of transition on the HAWT performance.

2 Methodology

2.1 Navier-Stokes Equation in rotating frame

For the rotating wind turbine simulation, letting the reference frame rotate with the blade allows one to avoid the complexity of moving mesh. Correspondingly , the Navier Stokes (NS) equations need to be modified to incorporate the Centrifugal and Coriolis effects of the rotating frame.
Let $\boldsymbol{u}$ denotes the velocity observed by a stationary observer (who is stationary with respect to the wind turbine mast), and $\boldsymbol{v}$ denotes the velocity observed by another observer who is rotating together with the reference frame (stationary with respect to the wind turbine blades).
$\boldsymbol{v}$ and $\boldsymbol{u}$ are related by:

$$\boldsymbol{u} = \boldsymbol{v} + \boldsymbol{\omega} \times \boldsymbol{r} \tag{1}$$

where $\boldsymbol{\omega}$ is the angular velocity vector and $\boldsymbol{r}$ is the position of fluid particle in rotating frame, where the center is located at the axis of rotation of the turbine. Since $\boldsymbol{u}$ is governed by Navier Stokes equations,

we can insert equation (1) to get the governing equations for $\boldsymbol{v}$. After some simplification, we have:

$$\nabla \cdot \boldsymbol{v} = 0 \tag{2}$$

$$\frac{\partial \boldsymbol{v}}{\partial t} + \boldsymbol{v} \cdot \nabla \boldsymbol{v} + \boldsymbol{\omega} \times (\boldsymbol{\omega} \times \boldsymbol{r}) + 2\boldsymbol{\omega} \times \boldsymbol{v} = -\nabla p + \nu \Delta \boldsymbol{v} \tag{3}$$

The form of mass equation is unchanged, but the Centrifugal term $\boldsymbol{\omega} \times (\boldsymbol{\omega} \times \boldsymbol{r})$, and Coriolis term $2\boldsymbol{\omega} \times \boldsymbol{v}$ arise in momentum equation because of the rotation.

The equations (2) and (3) are solved using the open source Spectral Element Method code Nek5000. which is based on high oder scheme and is highly scalable. For more information about the code, please refer to [2]. The calculations were performed on the French National Server named Institute for Development and Resources in Intensive Scientific Computing (IDRIS). IBM Blue Gene/Q was the super computer used and the total allocated CPU time for the project is about 5 millions hours.

2.2 LES model

LES requires less CPU time than Direct Numerical Simulation (DNS) because it only resolve the large scale motion of fluid, and leave the effect of small scale motion to be filtered. Since the small scale motions are mainly dissipative, an eddy viscosity can be added to the kinematic viscosity term in NS equation. Another way to account the small scale dissipative effect is through numerical dissipation, so no additional calculation of artificial viscosity is needed. This is referred as Implicit LES or Under-resolved DNS (UDNS). Here we call it UDNS.

In this paper, the LES model used is the classic Dynamic Smagrinsky model[3], which can be written as:

$$\nu_r = c_s(\Delta)^2 \overline{S} \tag{4}$$

ν_r is the eddy viscosity. Δ is the local grid scale. $\overline{S}$ is the magnitude of strain rate tensor S_{ij}. c_s is determined dynamically , see Lilly [4].

It is well known that the eddy viscosity calculated from the Smagrinsky model exhibit violent variation across the flow field, which can make the simulation unstable and eventually diverges [5]. Techniques were developed to tackle this drawback, such as cutting off the negative value, span-wise averaging, and Lagrangian averaging [6]. The span-wise averaging is only suitable for flows with a homogeneous direction such as channel flow, making it unsuitable for the current simulation. Lagrangian averaging is based on the idea that the eddy viscosity is convected by the fluid motion , just like a passive scalar, so an averaging can be done along the fluid particle trace. However, we found this techniques is unsuitable neither because the filtering in the Spectral Element Method (SEM) will cause mesh related pattern, which is not convective.

In oder to overcome this difficulty, an element-wise averaging technique is used. After having the ν_r at each spectral collocation point of an element, ν_r is averaged inside the element. Numerical experiments show that this technique allows stable calculations.

2.3 Validation case set-up

The validation case is a transitional flat plat boundary layer flow with zero pressure gradient. The computational domain is $1000\delta_0 \times 120\delta_0 \times 62.24\delta_0$ in x, y and z directions, where the δ_0 is the displacement thickness at the inlet x_0. The Reynolds number Re_{δ_0} based on δ_0 is 650.

Three cases with the same flow parameter but different meshes or settings are carried out. The first case,

which we refer to DNS, has an element number of $240 \times 40 \times 32$ in x, y and z directions respectively, which ensures a fully resolved DNS with a spatial resolution of $\Delta y^+_{min} = 1$, $\Delta x^+ = 20$ and $\Delta z^+ = 10$. The LES uses a grid 2 times coarser with $120 \times 20 \times 16$ elements, leading to a spatial resolution of $\Delta y^+_{min} = 2$, $\Delta x^+ = 20$ and $\Delta z^+ = 40$. The under-resolved DNS case uses the same mesh (resolution) as LES but with the eddy viscosity model turned off. For all the calculations, $8 \times 8 \times 8$ spectral collocation points are used inside a single element.

Blasius profile is used as initial condition. Disturbance is introduced by wall suction/blowing. At $50 <$

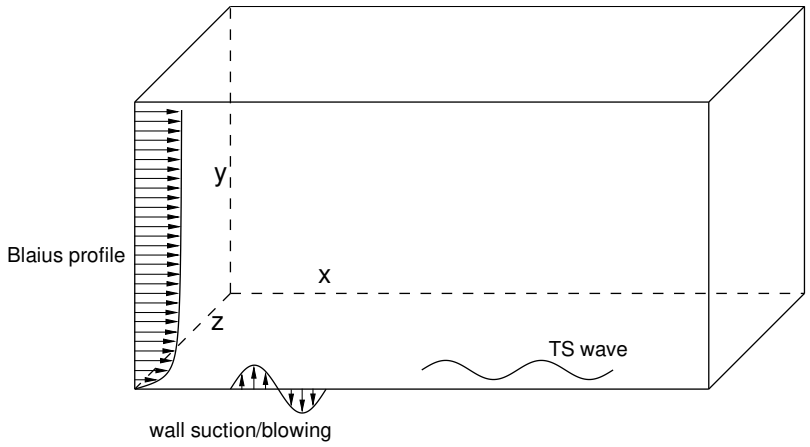

Figure 1: Numerical domain for the flat plate simulation (not to scale)

$x < 85$, the wall-normal velocity v at the boundary is specified as $0.01 \times sin[0.18(x-50)] \times cos(0.05t)$ + $0.001 \times sin(0.2z) \times sin(0.05t)$. The first term corresponds to a 2D harmonic disturbance while the second term introduces some non-uniformity in span-wise direction. The wave-number 0.18 and frequency 0.05 are chosen such that it matches with Tollmien-Schlichting waves. As we will see in the next section, this kind of disturbance will develop into TS wave downstream, and intrigue laminar-turbulent transition. Figure 1 gives an illustrative figure of the set-up.

2.4 Turbine Model set-up

The model under investigation is the LM38.8m blade with a 1.24 meter extension at root. There exist an extensive field and wind tunnel experiment results for this blade. The sections of LM38.8m blade consist of a series of NACA63-4XX (XX is max thickness) airfoil with different thicknesses and chord lengths, and a transition region near the root. The total blade span is 40m. Figure $6a$ shows the model under investigation. The blade span is aligned with y axis. The incoming flow is towards the positive z axis. The blade is rotating with a positive angular velocity in z component.

With our computational capacity, it is unable to resolve the whole blades. So the simulated domain is restricted from 15m to 35m of the blade span. The mesh is more concentrated in the middle of the span as shown by $2c$, which refers as 'Resolved portion' in figure $6a$. In this region, the spatial resolution in the x and y directions are constant, which ensures a fully resolved LES.Figure $6b$ gives boundary conditions. Since the blade is truncated in the span-wise direction, it is not possible to define a physical boundary condition for the two boundary surface at the span ends. A simple velocity Dirichlet boundary condition is imposed. Hence, the blade tip and root are not analyzed. Figure $2d$ shows a cut plane of

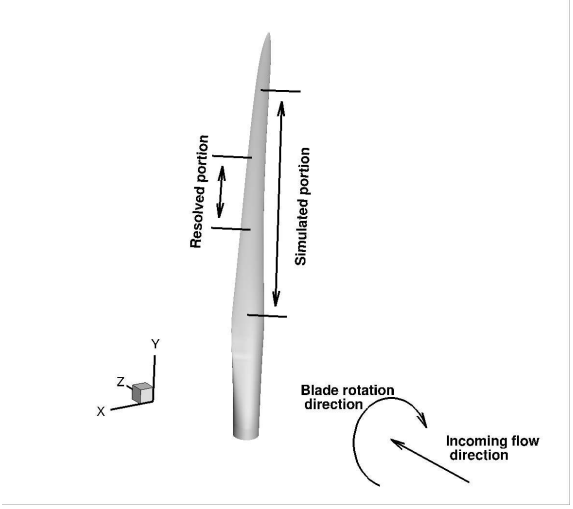

(a) Wind turbine blade set up and simulation area

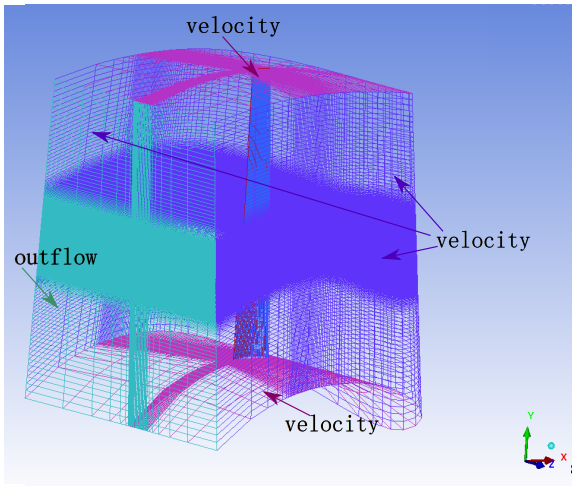

(b) DNS domain and Boundary conditions

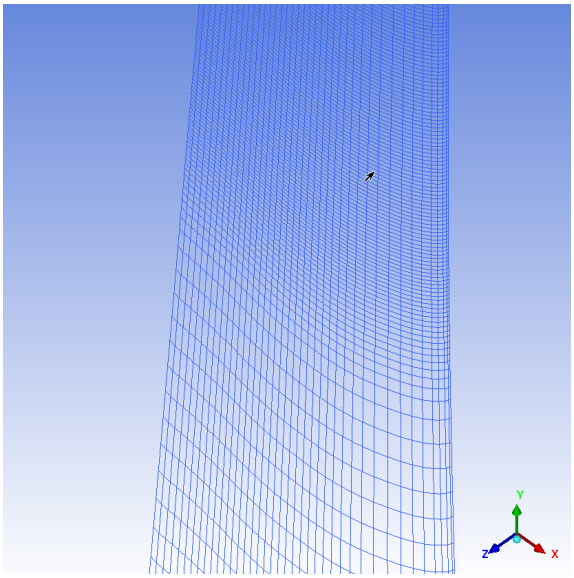

(c) Mesh at the blade surface

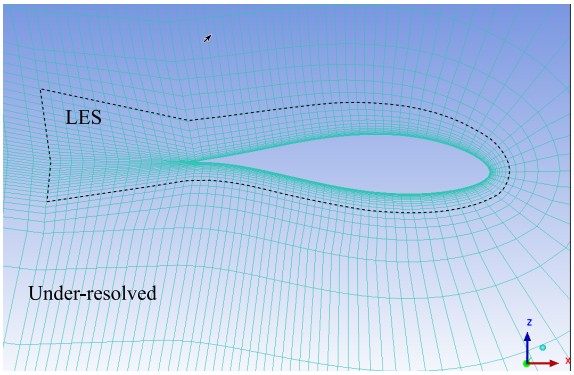

(d) Mesh of the NACA63-4XX section

Figure 2: Set-ups for the blade simulation

the mesh. Refinments are performed near the blade surface and in the near wake to obtain a correct spatial resolution near the blade. The total number of element is around 0.67 million, which gives about 0.23 billion grid points if the 8th order spectral is used in each element. The operating conditions are an upstream velocity of $V_\infty = 6$m/s and a Tip Speed Ratio $TSR = \frac{\omega R}{V_\infty} = 8$, where R is the radius of the turbine. To perform LES, the Reynolds number had to be decrease by increasing artificially the laminar kinematic viscosity in the DNS code. The average chord Reynolds number simulated is around 0.3 million near the middle span, which is 1/10th of the full scale turbine Reynolds number (i.e. around 3 millions). The simulated Reynolds number was set in order to induce similar laminar to turbulent transition on both sides of the blade. The simulation is started using 6th oder. When the flow is stabilized, the order is increased to 8th until full physical convergence of the boundary layer flow. The LES model is then activated, and physical convergence is performed again.

3 Results

3.1 LES model validation

After some adjustment, the disturbance evolves to TS wave behind the suction/blowing location. Because the amplitude of disturbance (0.01) is relative large, the TS wave enters nonlinear stage quite early. Figure 3 shows the instantaneous iso-contour of wall normal velocity for the DNS and LES results. The Λ vortex structure can be clearly identified around $x = 200$ in DNS result, showing a typical H-type transition. Further downstream, the Λ structure breakdown and the flow becomes turbulent. For the LES result, although the Λ vortex structure is not as clear as the DNS, it is identifiable and the LES clearly captures the transition to turbulence with the same mechanism, and also captures the turbulent structures downstream.

The friction coefficient is given in Figure 4. The laminar-turbulent transition happens around $x = 200$, where the friction coefficient cf experiences a large increases. At $x = 300$, All the simulations overshoot that of -1/7 law of turbulent boundary layer, which is an evidence of H-type transition [8]. Compared with under-resolved DNS, the LES result is closer to the DNS in both the transitional and the turbulent regions. Please note that these friction coefficients are not fully averaged in time, and smoother curves will be presented in the final version of the paper.

Figure 5 compares the mean profiles and Root Mean Squared (RMS) at $x = 380$ and $x = 600$ with the

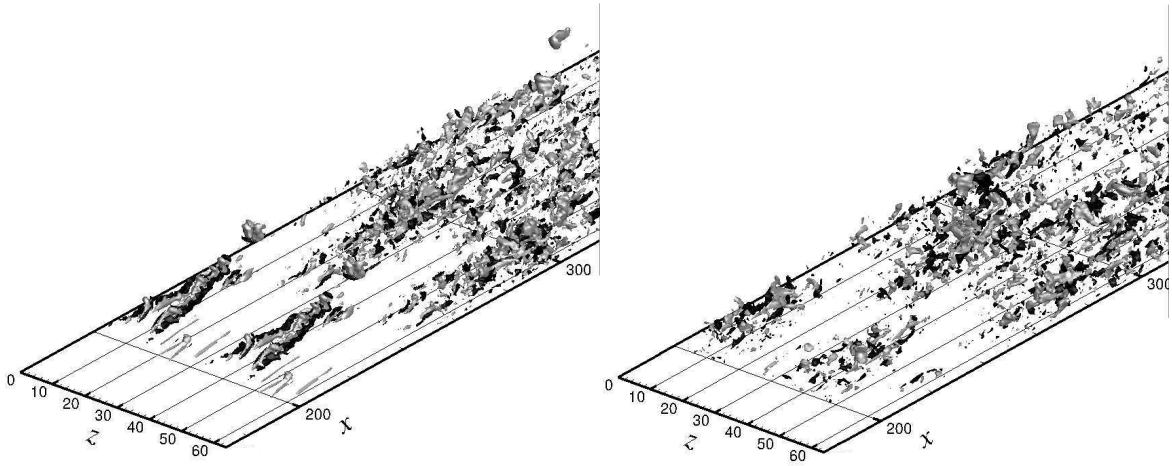

(a) (b)

Figure 3: iso-coutour of v, the dark region is $v = -0.1$, and the light region is $v = 0.1$ (a)DNS, (b)LES

DNS result from[11]. For the DNS, the momentum thickness θ at $x = 380$ is 1.02, which corresponds to $Re_\theta = 670$, and $Re_\theta = 1000$ at $x = 600$. Overall, Both DNS and LES agree well with the result from literatures, while the under-resolved DNS results departure from DNS in the buffer region and log-law region.

3.2 Wind turbine blade boundary layer flow

The turbine blade results are obtained quite recently and are still under post-processing and analysis. The comparison of the results obtained by the under resolved DNS at 6th and 8th ordrer as well as the

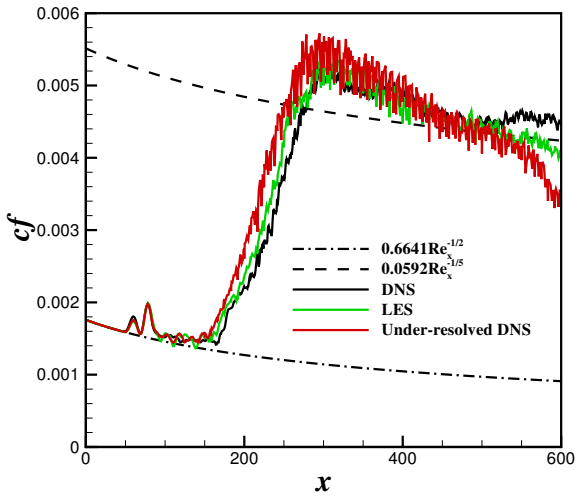

Figure 4: Friction coeficients, the red line is from blasius profile, and the blue line is from -1/7 law

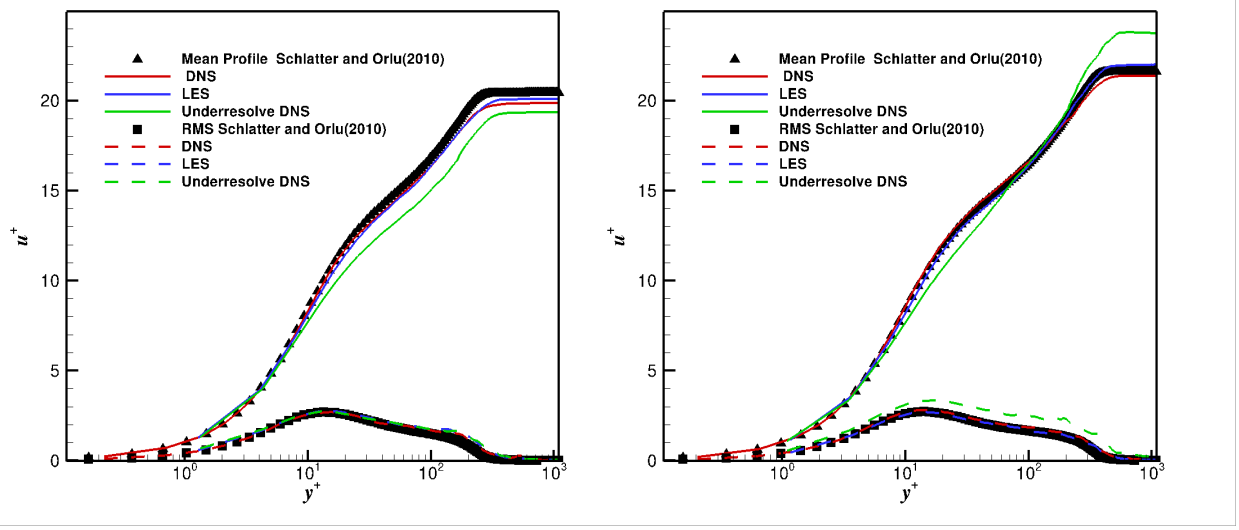

(a) (b)

Figure 5: Comparision of mean profile (solid lines) and RMS (dashed line) with that from [11](a) $Re_\theta = 670$, (b) $Re_\theta = 1000$

fully resolved LES at 8th order will be presented in the final version of the paper. Figure 6 shows the λ_2 criterion obtained by the UDNS at order 8th on the pressure and suction sides of the resolved portion, see Figure 6a. The chord-wise direction is made non dimensionnal, where $x/c = 0$ corresponds to the leading edge of the blade and $x/c = 1$ corresponds to the trailing edge. The λ_2 structures on the pressure side is clearly identifiable, which indicates that the transition is intrigued by 2D Tollmien–Schlichting wave starting at $x/c = 0.75$ from the leading edge (at $x/c = 0$), followed by a progressive development of 3D boundary layer flow which form hairpin structures around $x/c = 0.85$, and then cause turbulent boundary layer development up to trailing edge. At the suction side, because of higher adverse pressure gradient, the transition occurs much closer to the leading edge and is more brutal, which induces turbulent boundary layer along half of the chord. The transition region is seen to be induced by a different

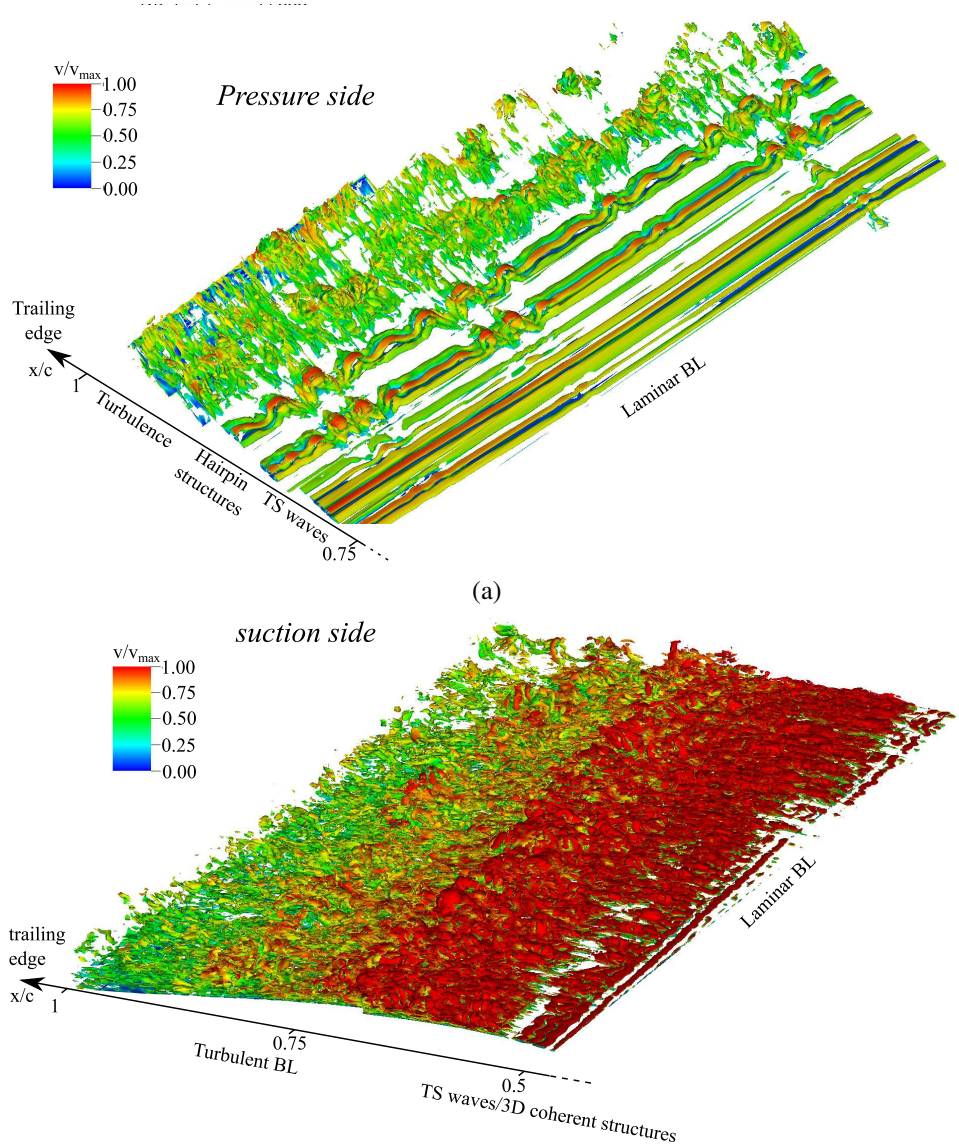

Figure 6: Iso λ_2 with velocity contours at (a) pressure side, (b) suction side in the resolved portion obtained with th UDNS at 8th order.

mechanism, that seems to change depending on the span-wise location. The possible reasons are (1) the centrifugal forces that increases at we get close to the tip, and induces cross flow effects, (2) the local Reynolds number, which is not constant for a given x location and modify the scales of coherent and turbulent structures and (3) the Under-resolved DNS, which is not able to fully capture the mechanism of transition. The upcoming results from the LES simulation should enhence the analysis of transition at the suction side.

4 Conclusion

In this paper, the laminar to turbulent transition is simulated on a wind turbine blade with the full effect of turbine rotation, using the spectral element code Nek5000. The boundary layer flow is resolved on a portion of the blade span because of the limited computational ressources. A LES method based on the dynamic Smagrinsky model with an element-wise averaging technique is introduced. It is first validated

on a transitional flat plate boundary layer. The H-type transition is correctly captured by the LES, and the results agree well with the litterature, based on the wall friction coefficient, the boundary layer profiles and RMS. The first results obtained with under-resolved DNS at 8th order are then presented. It shows different mechanism of transition at the pressure and suction sides of the blades. Whereas the pressure side is characterized by classical TS waves, followed by the formation of hairpin structures that cause the transition to turbulence, the suction side shows that a more complex mechanism may occurs, which still needs to be confirm by the fully resolved LES. This will be presented in the final version of the paper.

Acknowledgements

This work was performed using HPC resources of GENCI/IDRIS (Grant 2016-[100631]) at Orsay, France on the IBM Blue Gene/Q (Turing). Flow visualizations were made using the open-source software VisIt VisIt.

References

[1] H Aagaard Madsen, C Bak, U Schmidt Paulsen, M Gaunaa, P Fuglsang, J Romblad, NA Olesen, P Enevoldsen, J Laursen, and Leo Jensen. The dan-aero mw experiments: final report. *Danmarks Tekniske Universitet, Risø Nationallaboratoriet for Bæredygtig Energi, available at: orbit. dtu. dk*, 2010.

[2] Paul F Fischer, James W Lottes, and Stefan G Kerkemeier. nek5000 web page, 2008.

[3] Massimo Germano, Ugo Piomelli, Parviz Moin, and William H Cabot. A dynamic subgrid-scale eddy viscosity model. *Physics of Fluids A: Fluid Dynamics*, 3(7):1760–1765, 1991.

[4] Douglas K Lilly. A proposed modification of the germano subgrid-scale closure method. *Physics of Fluids A: Fluid Dynamics*, 4(3):633–635, 1992.

[5] Stephen B Pope. Turbulent flows, 2001.

[6] Charles Meneveau, Thomas S Lund, and William H Cabot. A lagrangian dynamic subgrid-scale model of turbulence. *Journal of fluid mechanics*, 319:353–385, 1996.

[7] Antoine Ducoin, J-Ch Loiseau, and J-Ch Robinet. Numerical investigation of the interaction between laminar to turbulent transition and the wake of an airfoil. *European Journal of Mechanics-B/Fluids*, 57:231–248, 2016.

[8] T Sayadi and P Moin. Predicting natural transition using large eddy simulation. *Center for Turbulence Research Annual Research Briefs*, pages 97–108, 2011.

[9] Shamsoddin, Sina and Porté-Agel, Fernando. Large eddy simulation of vertical axis wind turbine wakes. *Energies*, pages 890–912, 2014.

[10] Martínez-Tossas, Luis A and Churchfield, Matthew J and Leonardi, Stefano. Large eddy simulations of the flow past wind turbines: actuator line and disk modeling. *Wind Energy*, pages 1047–1060, 2015.

[11] Philipp Schlatter and Ramis Örlü. Assessment of direct numerical simulation data of turbulent boundary layers. *Journal of Fluid Mechanics*, 659:116–126, 2010.

[12] Li, Yuwei and Paik, Kwang-Jun and Xing, Tao and Carrica, Pablo M. Dynamic overset CFD simulations of wind turbine aerodynamics. *Renewable Energy*, pages 285–298, 2012.

[13] Abuan, Binoe E and Howell, Robert J. The performance and hydrodynamics in unsteady flow of a horizontal axis tidal turbine. *Renewable Energy*, pages 1338–1351, 2019.

[14] Johansen, Jeppe and Sørensen, Niels N and Michelsen, JA and Schreck, S. Detached-eddy simulation of flow around the NREL Phase VI blade. *Wind Energy: An International Journal for Progress and Applications in Wind Power Conversion Technology*, pages 185–197, 2002.